A paralogue of the phosphomutase-like gene family in *Candida glabrata*, *Cg*Pmu2, gained broad-range phosphatase activity due to a small number of clustered substitutions

Kelly A. Orlando*, Christine L. Iosue†, Sarah G. Leone†, Danielle L. Davies† and Dennis D. Wykoff†[1]

*Department of Biology, Immaculata University, Immaculata, PA 19345, U.S.A.
†Department of Biology, Villanova University, Villanova, PA 19085, U.S.A.

Inorganic phosphate is required for a range of cellular processes, such as DNA/RNA synthesis and intracellular signalling. The phosphate starvation-inducible phosphatase activity of *Candida glabrata* is encoded by the gene *CgPMU2* (*C. glabrata* phosphomutase-like protein). *CgPMU2* is part of a three-gene family (∼75 % identical) created through gene duplication in the *C. glabrata* clade; only *Cg*Pmu2 is a PHO-regulated broad range acid phosphatase. We identified amino acids that confer broad range phosphatase activity on *Cg*Pmu2 by creating fusions of sections of *CgPMU2* with *CgPMU1*, a paralogue with little broad range phosphatase activity. We used site-directed mutagenesis on various fusions to sequentially convert *Cg*Pmu1 to *Cg*Pmu2. Based on molecular modelling of the Pmu proteins on to a histidine phosphatase crystal structure, clusters of amino acids were found in two distinct regions that were able to confer phosphatase activity. Substitutions in these two regions together conferred broad phosphatase activity on *Cg*Pmu1. Interestingly, one change is a histidine adjacent to the active site histidine of *Cg*Pmu2 and it exhibits a novel ability to partially replace the conserved active site histidine in *Cg*Pmu2. Additionally, a second amino acid change was able to confer nt phosphatase activity to *Cg*Pmu1, suggesting single amino acid changes neofunctionalize *Cg*Pmu2.

Key words: *Candida glabrata*, histidine, PHO pathway, phosphatase, site-directed mutagenesis.

INTRODUCTION

Inorganic phosphates are required for a wide range of cellular processes, such as DNA/RNA synthesis and intracellular signalling. In multicellular organisms such as humans, inorganic phosphate concentration in blood plasma is regulated by the endocrine system and excess phosphate is excreted or stored in the vertebrate skeleton [1]. Single-celled organisms, such as the yeast species *Saccharomyces cerevisiae* and *Candida glabrata*, experience fluctuations in resource availability and without a stable phosphate storage system, they must adapt to external changes in inorganic phosphate on a cellular level. The capacity of a single-celled organism to adapt to changes in both the amount of environmental phosphate available and the organic phosphate source present can affect its ability to survive.

The *S. cerevisiae* the phosphate starvation pathway (PHO pathway) is a well-characterized mechanism for regulating phosphate intake [2]. The PHO pathway converges on the transcriptional regulation of approximately 20 genes during inorganic PHO, including up-regulation of the gene encoding an acid phosphatase, *PHO5* [3]. The Pho5 protein is then secreted into the periplasmic space, where it can cleave phosphate off of organic phosphate-containing molecules in the surrounding environment. This extracellular phosphatase activity can be readily observed through a colorimetric plate assay [4]. The related yeast species *C. glabrata*, which also exhibits phosphate starvation-inducible phosphatase activity, lost the *PHO5* gene [5]. We determined that *CgPMU2* (*C. glabrata* phosphomutase-like protein), part of a three-gene family created through gene duplication, neo-functionalized to functionally replace *PHO5* [4,6]. *CgPMU2* is up-regulated in response to phosphate starvation and can cleave phosphate off of a number of different phosphate-containing compounds, including glycerol phosphate, nucleotides and 1-naphthyl phosphate (1-NP) [4]. The homologue of the *Cg*Pmu proteins in *S. cerevisiae*, *Sc*Pmu1, was originally named a Pmu homologue because of its primary sequence similarity, especially in its active site, to phosphoglycerate mutases (PGMs) from a number of organisms [7]. However, although previous studies looking at the function of *Sc*Pmu1 have found that it could lower levels of a number of phosphorylated substrates [removing a phosphate from trehalose-6-phosphate and removing a phosphate from AICAR (5-phosphoribosyl-4-carboxamide-5-aminoimidazole), a toxic intermediate in the purine and histidine synthesis pathways], it is unclear whether it can act as a phosphomutase in those reactions [7–9]. In our own previous study, we determined that all three members of the *Cg*Pmu family are able to remove phosphate from a few substrates *in vitro* but only CgPmu2 is induced under phosphate-starvation conditions and is able to remove appreciable amounts of phosphate from 1-NP in an *in vivo* assay [4]. Therefore, we hypothesize the ancestral *Cg*Pmu1 protein duplicated and then one of the paralogues accumulated mutations allowing it to function as a more broad-based phosphatase functionally replacing the missing Pho5 protein. To further support this hypothesis, we have previously demonstrated that the *PMU2* promoter has accumulated mutations to become phosphate regulated [10]. Although the primary amino acid sequences of *Sc*Pho5 and *Sc*Pmu1 share little similarity, they are both members of the

Abbreviations: *Cg*Pmu, *Candida glabrata* phosphomutase-like protein; dPGM, cofactor-dependent phosphoglycerate mutase; G-1-P, glycerol-1-phosphate; 1-NP, 1-naphthyl phosphate; PGM, phosphoglycerate mutase; PNPP, *p*-nitrophenylphosphate.

[1] To whom correspondence should be addressed (email dennis.wykoff@villanova.edu).

histidine phosphatase superfamily [11]. This family is so named because the conserved catalytic core of amino acids in the active site includes a histidine which becomes phosphorylated during hydrolysis [11]. Members of the histidine phosphatase superfamily of enzymes have little primary sequence similarity, but they all contain a core β-sheet supporting the catalytic core, with a number of key conserved active site amino acids [11].

In the present study, we show that members of the *Cg*Pmu protein family retain the conserved catalytic core amino acids of the histidine phosphatase superfamily. We then set out to identify the amino acids that confer novel phosphatase activity on *Cg*Pmu2, using various phosphate-containing substrates. We created fusions of sections of *Cg*Pmu2 with the putative ancestral protein, *Cg*Pmu1, which has little broad range phosphatase activity. This method prompted us to focus on the C-terminal portion of the protein and to use site-directed mutagenesis on fusions to sequentially convert *Cg*Pmu1 to *Cg*Pmu2. Using these methods, we identified point mutations that contribute to the broad range phosphatase activity of *Cg*Pmu2. This mutational analysis identified a novel redundant histidine adjacent to the active-site histidine in *Cg*Pmu2 that has not been observed in any member of the histidine phosphatase superfamily. Additionally, we identified a single mutation that allows for *in vivo* hydrolysis of phosphate from a nucleotide, allowing for the exploration of selectively advantageous single amino acid changes.

MATERIALS AND METHODS

Strain construction

To generate the *CgPMU1-PMU2* fusion constructs, the sequences for both genes were aligned and divided into roughly four regions, where the divisions were determined by regions of high sequence conservation (Figure 1A). Primers were designed for the 5′- and 3′-ends of each region, with half homology to *PMU1* and half homology to *PMU2* (primer sequences are available upon request). Regions of *PMU1* and *PMU2* were amplified and then two or three PCR products were combined according to the schematic in Figure 2A and amplified using the appropriate outermost primers which have homology to either the *PHO5* promoter or the *YFP* in the plasmid. These fusion products, containing a full-length gene made up of *PMU1* and *PMU2*, were cloned by homologous recombination into a *PHO5*p-*Pac*I-*YFP*-pRS313 (*HIS3*) plasmid using a standard lithium acetate transformation [12,13]. The plasmids were then transformed into a *Cgpmu2*Δ strain [4] to determine whether the fusion constructs can complement phosphatase activity.

To perform site-directed mutagenesis to convert *CgPMU1* to *CgPMU2*, primers were designed with homology to *CgPMU1* but with base pairs to mutate the amino acid in *PMU1* to the corresponding amino acid in *PMU2*. The two PCR products, both the 5′- and 3′-ends of the gene, were combined and amplified using the appropriate outermost primers which have homology to either the *PHO5* promoter or *YFP* in the plasmid. These fusion products were cloned as previously described [12]. All plasmids introduce a stop codon prior to the *YFP* ORF. Each mutant plasmid was sequence verified.

Growth medium

Yeast strains were grown in YEPD medium or SD medium made with complete supplement mixture (CSM) without histidine [6] (Sunrise Science Products). To measure acid phosphatase activity, strains were grown in SD medium without histidine that was also lacking inorganic phosphate.

Structure analysis

The *C. glabrata* Pmu1 and Pmu2 sequences were each submitted to Phyre2 for structure prediction; the PDB crystal structure C4embD was the first result for CgPmu1 and the third result for CgPmu2, with both having a 100 % confidence and having a 22 % and 21 % identity respectively. C4embD is the PGM from *Borrelia burgdorferi*. Their predicted structures were visualized using Swiss-Pdb Viewer 4.1.0.

Assay for phosphatase activity

For a semi-quantitative assay of phosphatase activity *in vivo*, agar plates with colonies grown in phosphate starvation conditions for ∼24 h were overlaid with Fast Blue Salt B stain, 1-NP and 0.1 M sodium acetate (pH 4.2) [14]. When phosphate is cleaved from 1-NP, it reacts with Fast Blue Salt B to form a red colour, causing the yeast colony to turn red when there is extracellular 1-NP phosphatase activity and to remain white when there is little activity.

For a quantitative assay of phosphatase activity *in vivo*, hydrolysis of *p*-nitrophenylphosphate (PNPP) was measured. Strains were grown in high phosphate conditions at 30 °C overnight. Cells were washed with sterile water and inoculated into SD medium that was lacking inorganic phosphate and grown at 30 °C overnight. One millilitre of cells (OD_{600} ∼ 0.5) were pelleted by centrifugation and resuspended in sterile water. Cells were incubated with 10 mM PNPP at pH 4.2 at 25 °C for 10 min. The reaction was quenched with saturated Na_2CO_3. Phosphatase activity was measured in units expressed as OD_{400}/OD_{600} [15].

Hydrolysis of GMP

To measure hydrolysis of GMP *in vivo*, cells were grown in high phosphate conditions at 30 °C overnight. Cells were washed with sterile water and inoculated into SD medium that was lacking inorganic phosphate but had 5 mM GMP added as the sole source of phosphate. Triplicate cultures were inoculated at the same OD_{600} (0.05) and grown at 30 °C for 24 h. OD_{600} was measured after 24 h.

Bacterial expression and purification of *Cg*Pmu1–Pmu2 fusions and mutants

*Cg*Pmu1–Pmu2 fusions and mutants were amplified by PCR, digested with *Bam*HI and/or *Xho*I and ligated into a pET16b vector. Clones were confirmed by sequencing and transformed into C3013H *Escherichia coli* cells (New England Biolabs). Pooled transformants were grown at 30 °C and induced with 1mM IPTG for 2 h. Cells were lysed by sonication in 10 % glycerol, 50 mm Tris (pH 8), 250 mm NaCl, 0.1 % NP-40 (or Tween 20), 10 mm imidazole (pH 8), 1 mm 2-mercaptoethanol and protease inhibitors (Sigma Life Sciences). The N-terminal His_{10} tagged proteins were purified by immobilized metal affinity chromatography. Iminodiacetic acid resin (Sigma–Aldrich) was charged with cobalt chloride, loaded with cell extract and washed with the same buffer until no protein was detected in the flow through. The tagged proteins were eluted with 20 mM EDTA and dialysed overnight in lysis buffer. The total concentration of protein in the extract was determined by Bradford assay.

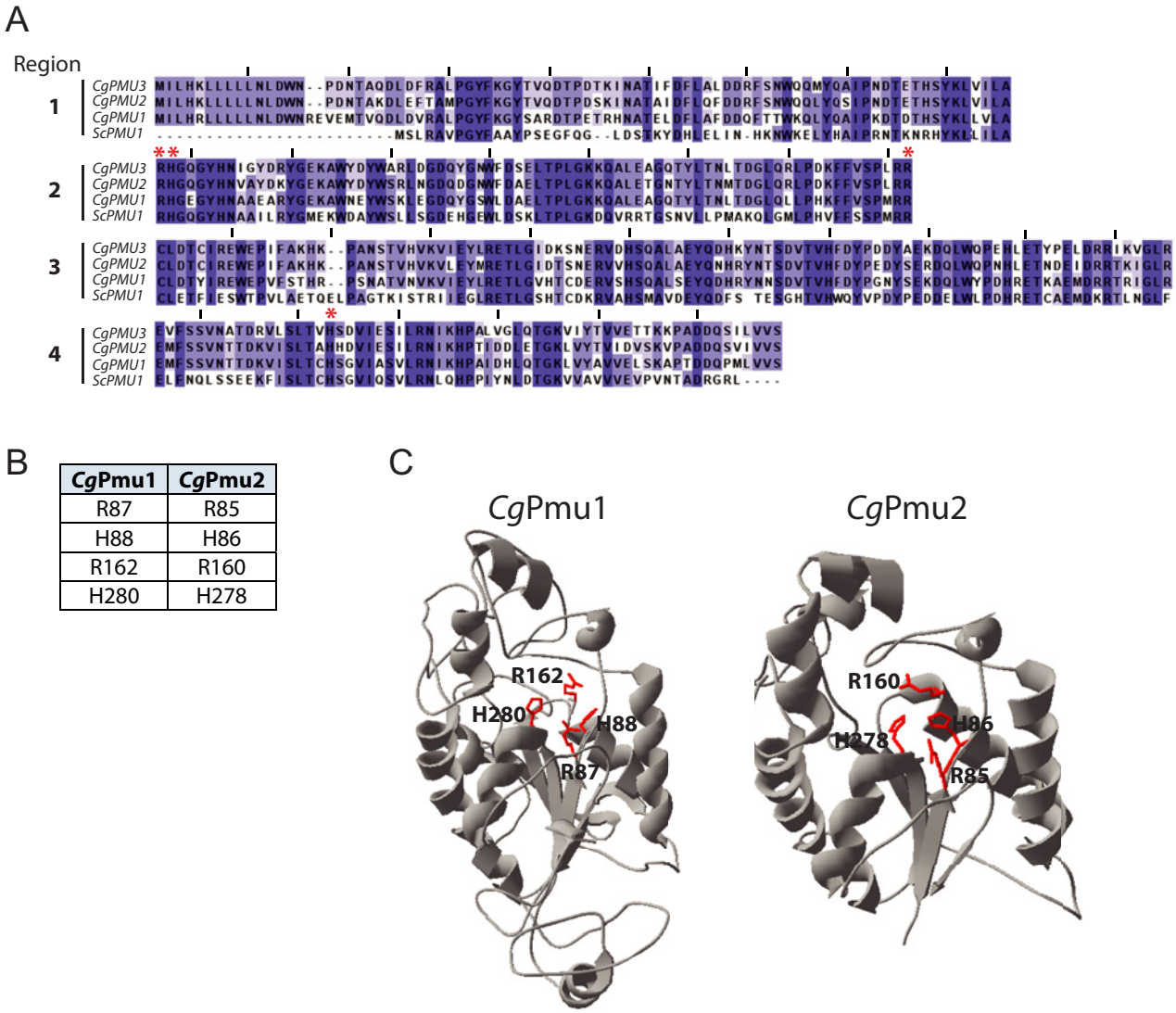

Figure 1 ***CgPMU2*** **and the ancestral gene** ***CgPMU1*** **show amino acid conservation in the active site**

(**A**) Sequence alignment of *C. glabrata* and *S. cerevisiae* Pmu proteins, showing conserved amino acids, constructed using Jalview v2.8.0b1 [28]. Dark blue represents amino acids that are conserved among all four proteins, medium blue those conserved between three of the proteins and light blue those conserved between two proteins. The alignment is divided into four rows, with each dividing point being areas of high similarity; from top to bottom the regions are labelled 1 through 4. Red asterisks represent active site amino acids. (**B**) Table listing the four active site amino acids in *Cg*Pmu1 and *Cg*Pmu2; H, histidine, R, arginine. (**C**) The *Cg*Pmu1 and *Cg*Pmu2 protein sequences were entered into the structure prediction website Phyre2 and one of the top results for both (c4embD) was a PGM from *Borrelia burgdoferi*. The predicted structures were visualized in ribbon form using DeepView/Swiss-PdbViewer, v4.1.0 [29]. Active site amino acids are labelled and highlighted in red for both *Cg*Pmu1 and *Cg*Pmu2.

Detection of phosphatase activity *in vitro*: phosphate released

To determine the specificity of each enzyme, the purified proteins were incubated with various phosphate-containing substrates for 20 min at 25 °C. Using 2-fold dilutions, the kinetics of each reaction were observed. PNPP was tested at concentrations ranging from 10 to 0.313 mM. GMP was tested at concentrations ranging from 15 to 0.469 mM. Glycerol-1-phosphate (G-1-P) was tested at concentrations ranging from 100 to 3.13 mM. The amount of phosphate released was quantified by incubating the reactions with 300 μl of Brilliant Green phosphate dye in a final volume of 1 ml at 30 °C for 30 min [16]. Phosphate released was measured in units of OD_{639} and reactions with and without enzyme were compared. Data were normalized using a standard curve with known amounts of inorganic phosphate (KH_2PO_4) and by subtracting a sample with no protein added. V_{max} and K_M values were calculated using a simulation in Excel to minimize error with a least-squares method. If we did not observe consistent Michaelis–Menten kinetics, then the measurement was considered not detected. We were unable to measure 1-NP activity because of interfering levels of inorganic phosphate.

RESULTS

CgPMU2 and the ancestral gene *CgPMU1* show amino acid conservation in the active site

In the *C. glabrata* clade, *PMU1* has undergone two duplication events post speciation from *Saccharomyces* and consequently *C.*

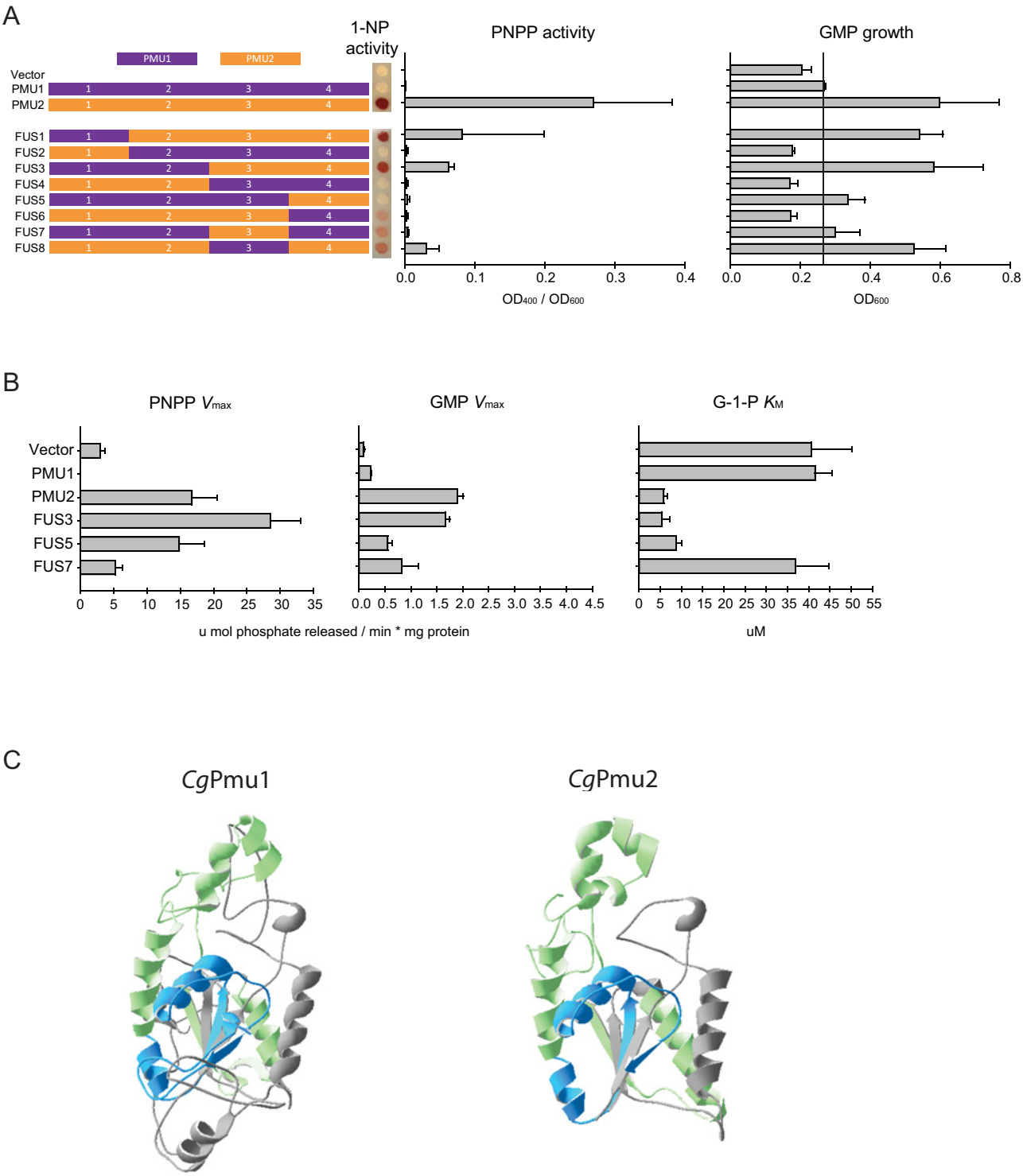

Figure 2 Regions 3 and 4 of Pmu2 confer phosphatase activity in Pmu1–Pmu2 fusions

(**A**) Schematic of Pmu1–Pmu2 fusions, with corresponding *in vivo* phosphatase activity results. Regions of *CgPMU1* (purple) or *CgPMU2* (orange) were combined as shown in the schematic and expressed in a *CgPMU2* deletion strain (*Cgpmu2*Δ) which has no detectable phosphatase activity ('Materials and Methods' for strain construction). 1-NP activity was assayed on cells growing in phosphate starvation conditions on an agar plate; red colour indicates 1-NP phosphatase activity. Adjacent bar graph (PNPP activity) represents whole cell assay of PNPP hydrolysis during phosphate starvation. *y*-axis represents the various fusions tested (same order as in the schematic). Activity was normalized to cell density and expressed as OD_{400}/OD_{600}. Bar graph on the right (GMP growth) represents whole cell assay of overnight growth with GMP as the sole phosphate source. *y*-axis is the same as PNPP activity. Activity is expressed as cell growth (OD_{600}). The vertical line represents the OD_{600} of *Cg*Pmu1. PNPP activity and GMP growth assays were performed in biological triplicate, with error bars representing standard deviation of the mean. (**B**) Purified proteins were incubated with various phosphate-containing substrates in *in vitro* kinetic assays: from left to right, the graphs represent the V_{max} of PNPP, V_{max} of GMP and the K_M of G-1-P. The amount of phosphate released was normalized using a standard curve of known inorganic phosphate. Experiments were performed in triplicate, with error bars representing the S.E.M. (**C**) Predicted structures of *Cg*Pmu1 (left) and *Cg*Pmu2 (right), with region 3 coloured green and region 4 coloured blue. Notice that a number of α-helices in region 3 rest above the active site region. Region 4 makes up part of the β-sheet underlying the active site.

glabrata and closely related species are the only species with a three gene *PMU* family [5]. The three Pmu proteins that are encoded by this gene family are approximately 75 % identical at the amino acid level and show a moderate level of amino acid conservation compared with the single Pmu1 protein expressed in *S. cerevisiae* (approximately 50 % identical; Figure 1A). All four enzymes contain the amino acids that make up the conserved catalytic core of the histidine phosphatase superfamily active site (red asterisks in Figure 1A): two arginines (R) and two histidines (H) [11]. When the protein structures of *Cg*Pmu1 and *Cg*Pmu2 were predicted using Phyre2 [17], the active site amino acids (listed in Figure 1B, highlighted in red in Figure 1C) mapped to the same region in both proteins (above the β-sheet twist) and corresponded to previously observed phosphatase and phosphomutase active site structures [11,18,19].

The C-terminal region of *Cg*Pmu2 is responsible for conferring phosphatase activity

Previously, we found that one of the *C. glabrata* proteins, *Cg*Pmu2, neofunctionalized to gain a high level of phosphate starvation-induced phosphatase activity [4]. We hypothesized that a limited number of amino acid changes in *Cg*Pmu1 could confer the increased phosphatase activity seen in *Cg*Pmu2. After aligning the amino acid sequences of the Pmu proteins, we divided them into four approximately equal parts, selecting regions of high conservation for the division points (Figure 1A). These points were selected so that fusion constructs combining the different regions of *Cg*Pmu1 and *Cg*Pmu2 could be produced through PCR (Figure 2A). These fusion constructs were inserted into plasmids and expressed in a *C. glabrata* strain lacking *CgPMU2* (*Cgpmu2*Δ), which has no detectable phosphatase activity. Using a colorimetric plate assay to measure 1-NP phosphatase activity during phosphate starvation, we determined that regions 3 and 4 of *Cg*Pmu2 (the C-terminus) conferred 1-NP phosphatase activity on *Cg*Pmu1 (Figure 2A). We also utilized two quantitative measures of *in vivo* phosphatase activity: hydrolysis of PNPP relative to cell density (PNPP activity) and growth in medium containing GMP as the sole source of phosphate to assess the ability to scavenge phosphate from nucleotides (GMP growth). The results of these assays complemented the 1-NP data for the most part, with the fusion containing the second half of *Cg*Pmu2 (FUS3) exhibiting an increased activity against PNPP and GMP. However, whereas region 4 alone had no effect on 1-NP activity and region 3 had a weak effect (FUS5 and FUS7), both had no effect on their own on *in vivo* PNPP activity and growth in GMP, suggesting some subtle changes in substrate specificity between the two regions. Overall our data demonstrate that the C-terminus of *Cg*Pmu2 is important for phosphatase activity. Both regions 3 and 4 seem to contribute to the gain in phosphatase activity seen in *Cg*Pmu2 (note activity of FUS3 compared with FUS5 or FUS7).

We cloned and purified His-tagged *Cg*Pmu1, *Cg*Pmu2, FUS3, FUS5 and FUS7 from bacteria to determine if the altered specificity we observed was a consequence of altered enzyme activity itself or an artefact of the variation between *in vivo* assays. We had previously observed that *Cg*Pmu1 and *Cg*Pmu2 differed in their K_M and/or V_{max} for various substrates [4]. For example, *Cg*Pmu2 had a much higher V_{max} than *Cg*Pmu1 for the substrate PNPP, whereas their K_M values for PNPP were similar. We also observed *Cg*Pmu2 had nucleotidase activity against GMP whereas *Cg*Pmu1 did not have detectable activity. Subjecting these purified proteins to kinetic analysis with PNPP, GMP and G-1-P demonstrated that replacing region 3 of Pmu1 with the Pmu2 sequence (FUS7) allowed for an incremental shift towards Pmu2 activity characteristics (Figure 2B). In addition, region 4 appears to be important for substrate specificity changes; transplanting just region 4 of Pmu2 into Pmu1 (FUS5) leads to a marked decrease in the K_M for G-1-P, a dramatic increase in V_{max} for PNPP and a smaller increase in V_{max} for GMP without a visible effect on 1-NP hydrolysis. It is worth pointing out that we found that the *in vitro* and *in vivo* characteristics of the FUS5 construct with regards to PNPP were conflicting (Figures 2A and 2B); the simplest explanation for this is that these isolated changes destabilize the enzyme in our *in vivo* PNPP phosphatase assay (see 'Discussion'). We conclude the amino acid residue(s) that contribute to the majority of Pmu2 activity and specificity are in regions 3 and 4.

When we mapped the four regions back to the predicted protein structures, we determined that in both proteins region 3 makes up one strand of the conserved β-sheet making up the core of the enzyme as well as a number of α-helices around and above the active site (Figure 2C, green ribbon). The predicted structures for the two proteins are similar in this region but not identical and the α-helices above the active site are connected to the rest of the protein by a less ordered stretch of amino acids. Rigden et al. [20] observed that this same region in *Bacillus stearothermophilus* PhoE had very few contact points with the rest of the protein; since this subdomain contains residues that line the active site, they hypothesized that it may be the key to PhoE's relatively broad specificity. Mikhailik et al. [19], when comparing two enzymes in the PGM/acid phosphatase family of enzymes, observed that one protein had a somewhat exposed active site whereas another contained a large stable region that covered the active site; they found that the one with the exposed active site could act on larger substrates, such as phosphorylated proteins. Therefore, it is possible that region 3 may contribute to phosphatase activity and/or substrate specificity by modifying how accessible the active site is to various substrates. Region 4 of the two proteins maps to a domain that contributes two strands of the core β-sheet (Figure 2C, blue ribbon), suggesting that it could play a key role in enzyme activity. Another possibility is that the C-terminal domain may affect the stability of the active site, which may affect whether the enzyme acts as a phosphomutase or a phosphatase, as has been previously seen with the enzyme dPGM (cofactor-dependent PGM) [21].

Amino acid changes near the active site can confer phosphatase activity on CgPmu1

Because we only observed a strong increase in 1-NP phosphatase activity when the entire C-terminal half of *Cg*Pmu2 was present in the fusion protein, we suspected that there was at least one set of amino acids each in region 3 and in region 4 that confer phosphatase activity on *Cg*Pmu2. Therefore, we created combinations of fusions containing one region of *Cg*Pmu2 in a *Cg*Pmu1 context with various point mutations, attempting to isolate the relative contribution of amino acids in each of the two C-terminal regions of the enzyme.

To determine the important amino acids in region 3, we began with the FUS5 construct, which contained regions 1–3 of *CgPMU1* and region 4 of *CgPMU2* and did not exhibit phosphatase activity against 1-NP on its own. We chose clusters of amino acids that differed in sequence between *Cg*Pmu1 and *Cg*Pmu2 in region 3 and named this group of amino acids the R3 mutants (Table 1). The R3 mutants are actually five amino acid changes in two sections of region 3 (R3a and R3b). When combined with region 4 of *Cg*Pmu2, the R3 mutants were able to confer phosphatase activity against both 1-NP and GMP *in vivo*,

Table 1 Amino acids involved in point mutations to convert *Cg*Pmu1 to *Cg*Pmu2

For each cluster of point mutations (region 3, region 4, adjacent histidine), the two columns on the right list the respective amino acids in *Cg*Pmu1 and *Cg*Pmu2. H (histidine), C (cysteine), D (aspartate), R (arginine), S (serine), N (asparagine), L (leucine), E (glutamate).

	Amino acids	
Mutation name	*Cg*Pmu1	*Cg*Pmu2
Region 3 mutations (R3a: H-D,C-S,D-N) (R3b: D-N, R-L)	His^{200}	Asp^{198}
	Cys^{202}	Ser^{200}
	Asp^{203}	Asn^{201}
	Asp^{245}	Asn^{243}
	Arg^{247}	Leu^{245}
Region 4 mutations (R4: A-E)	Ala^{285}	Glu^{283}
Adjacent His (H2) (S-H)	Ser^{281}	His^{279}

but not *in vivo* PNPP phosphatase activity (Figure 3A). All five amino acid changes were required for the full restoration of FUS3-like activity. *In vitro* kinetic assays showed that the R3 mutants plus region 4 of *Cg*Pmu2 (FUS5 + R3a + R3b) had the same high V_{max} for PNPP and GMP as fusions containing the entire regions 3 and 4 of *Cg*Pmu2 (FUS3), verifying the ability of the R3 mutants to confer the phosphatase activity observed in region 3 of *Cg*Pmu2 (Figure 3B).

To determine the amino acids that contribute to region 4, we combined a point mutation in region 4 with the FUS7 construct, which contained regions 1, 2 and 4 of *Cg*Pmu1 and region 3 of *Cg*Pmu2 and exhibited low phosphatase activity on its own (FUS7 + R4). A single point mutation in region 4 of the protein (Table 1) when combined with region 3 of *Cg*Pmu2, increased 1-NP phosphatase activity and *in vivo* hydrolysis of PNPP and GMP, relative to FUS7 (Figure 3A). These results were supported with the *in vitro* data. The *in vitro* data also demonstrated that the R4 mutation in the context of FUS7 (FUS7 + R4) was sufficient to alter the K_M of the protein for G-1-P to behave like *Cg*Pmu2 (Figure 3B). In Figure 3C, the predicted structures of both *Cg*Pmu1 wild-type and *Cg*Pmu1 with R3 and R4 alterations are drawn with the R3 and R4 amino acids highlighted in different colours and the amino acid side chains visible. Note that the amino acids in region 3 [Figure 3C, red (R3a) and blue (R3b)] are in areas of low-ordered structure connecting the catalytic core with a section of region 3 that sits above the active site; the low-ordered region could potentially function as a hinge to control the accessibility of substrates to the active site. The R4 amino acid (Figure 3C: yellow) is in an α-helix very close to the active site. Introduction of the R4 mutation into *Cg*Pmu1, a change from alanine (A) to glutamic acid (E), may affect the rigidity of the enzyme structure and potentially result in a change in activity. Alternatively, the introduction of glutamic acid may change charge interactions in the active site; regardless, this change increases the protein's affinity for G-1-P and increases the V_{max} for PNPP and GMP *in vitro*.

*Cg*Pmu2 has an additional histidine in the active site and this histidine is important for phosphatase activity

In the fusion experiments, we determined that the C-terminal region of *Cg*Pmu2 is important for phosphatase activity. In addition to the R4 mutant mentioned previously, we noticed an additional histidine (His^{279}) adjacent to the active-site histidine (His^{278}) in *Cg*Pmu2 that was not present in *Cg*Pmu1 (Figure 4A). To determine whether this histidine was involved in conferring phosphatase activity on *Cg*Pmu2, we made various *Cg*Pmu2 point mutants (Figure 4B). Mutation of the conserved histidine to alanine (H278A) in *Cg*Pmu2 eliminated almost all phosphatase activity; however, there was still a trace of 1-NP phosphatase activity (note the faint red in the 1-NP activity) indicating that the conserved His^{278} is not absolutely required for all phosphatase activity (Figure 4B). It was only when the adjacent histidine was also mutated (H278A, H279A) that we were able to completely block all phosphatase activity (Figure 4B). Cells retained phosphatase activity when only the adjacent *Cg*Pmu2 histidine (His^{279}) was mutated to an alanine, suggesting that the His^{278} is the main active site histidine but that this extra histidine (His^{279}) can take over as part of the catalytic core when His^{278} is missing.

We also added the adjacent histidine from *Cg*Pmu2 to *Cg*Pmu1 (S281H), but found that it was unable to confer phosphatase activity in the context of *Cg*Pmu1 (Figures 4B and 4C), indicating that the adjacent histidine is not sufficient for conferring the phosphatase activity of *Cg*Pmu2. However, because the R3 and R4 mutants only conferred increased phosphatase activity in combination with region 3 or region 4 of *Cg*Pmu2, we added the adjacent histidine to the FUS7 protein, which contains regions 1, 2 and 4 of *Cg*Pmu1 and region 3 of *Cg*Pmu2 (FUS7 + H2; Figure 5A). The S281H mutation, H2, in this context, conferred phosphatase activity against 1-NP, PNPP and GMP when combined with region 3 of *Cg*Pmu2 (Figures 5A and 5B). In fact, this additional histidine in the catalytic core behaves almost identically with the R4 mutational change (compare Figures 3A, 3B, 5A and 5B). When the predicted structures of the active site amino acids of *Cg*Pmu1 and *Cg*Pmu2 are mapped (Figure 4C, catalytic core residues in red), it is clear that the adjacent histidine (His^{279}), whereas not in the same orientation as the active site histidine (His^{278}), is located within the active-site pocket. We conclude that alterations in the active site either by S281H (H2) or A285E (R4) cause the *Cg*Pmu1 enzyme to behave much like the *Cg*Pmu2 enzyme. The only real difference is the enzyme activity in the *in vivo* PNPP assay, which might indicate a less stable protein under physiological conditions.

A combination of region 3 and region 4 point mutations are sufficient to confer phosphatase activity on *Cg*Pmu1

To determine how each point mutation contributes to the novel phosphatase activity of *Cg*Pmu2, we introduced various combinations of point mutations (R3, R4 and adjacent histidine) into *Cg*Pmu1 (Figure 6A). None of the point mutations alone had any effect on *Cg*Pmu1 1-NP phosphatase activity, but we found that various combinations of the mutations could confer phosphatase activity against 1-NP and GMP. The R4 change seems to be important for hydrolysis of GMP; all combinations of point mutations containing the region 4 substitution were able to grow in the presence of GMP (Figure 6A). Remarkably, the single A285E (R4) change conferred on *Cg*Pmu1 the ability to scavenge phosphate from GMP *in vivo* at nearly the same level as full-length *Cg*Pmu2 and raised the V_{max} to a similar level as *Cg*Pmu2 in *in vitro* assays with PNPP and GMP (Figures 6A and 6B). These results indicate that a single change might allow for a selective advantage, i.e. there could be a simple mutational change that alters the activity towards organic phosphates.

Combinations that conferred broader-range phosphatase activity always contained both groups of R3 changes (R3a and R3b) as well as H2 (adjacent histidine), R4 or both. The combination of all point mutations (PMU1 + R3a + R3b + H2 + R4 in Figures 6A and 6B) resulted in phosphatase activity

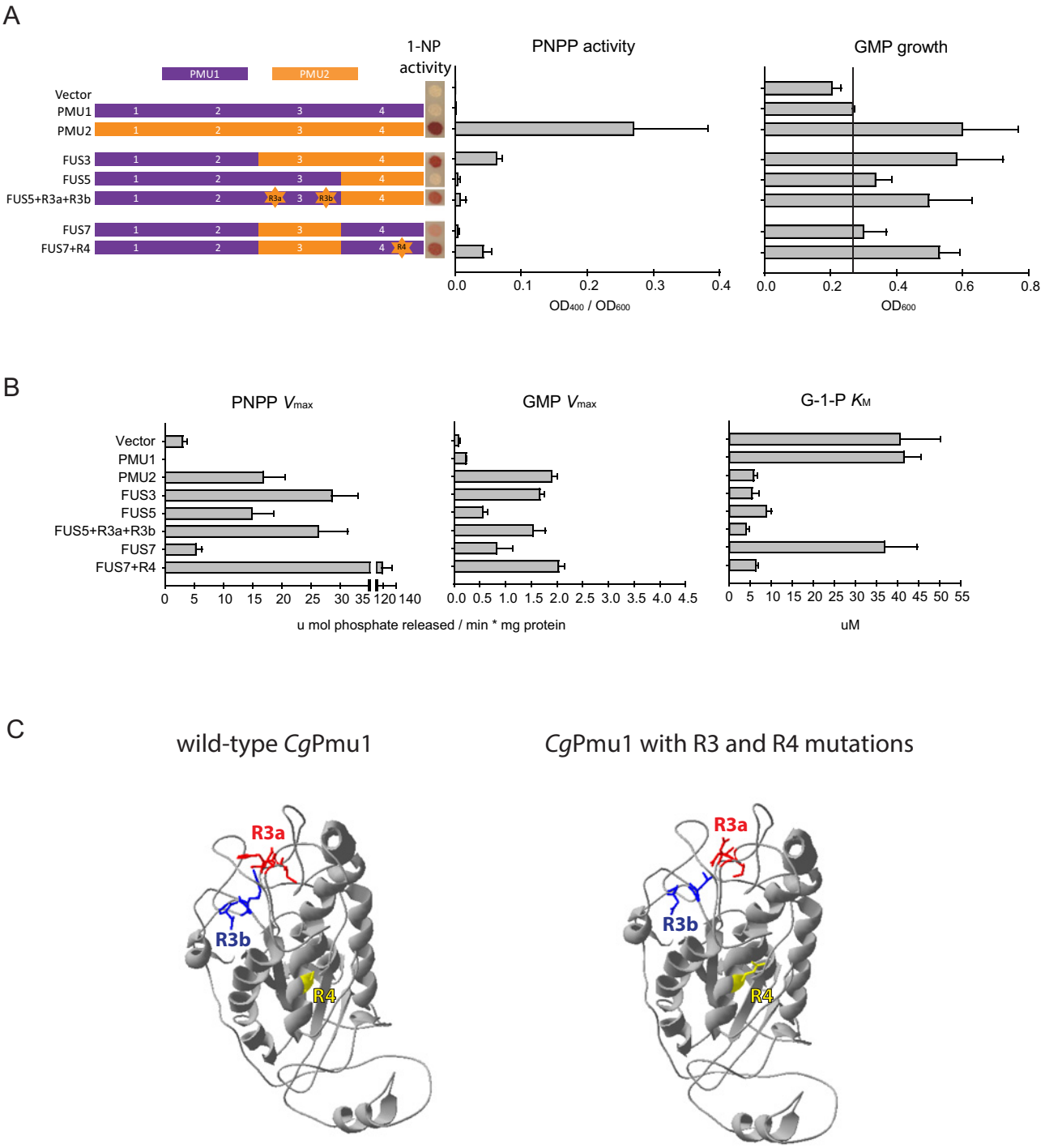

Figure 3 Point mutations in regions 3 and 4 of the protein are important for phosphatase activity

(**A**) Schematic of Pmu1–Pmu2 fusions plus point mutations, with corresponding *in vivo* phosphatase assay results. Clusters of point mutations (see Table 1 for specific amino acids mutated) were introduced into Pmu1–Pmu2 fusions (Figure 2A) in regions of Pmu1 sequence to convert the amino acid to that of the corresponding amino acid in Pmu2. *In vivo* phosphatase activity was measured as in Figure 2(A). Introduction of the R3 point mutations in a FUS5 background conferred phosphatase activity above FUS5 alone. Introduction of the R4 point mutation in a FUS7 background also conferred phosphatase activity above FUS7 alone. (**B**) Purified proteins were incubated with various phosphate-containing substrates in *in vitro* kinetic assays and measured as in Figure 2(B). (**C**) Predicted structures of wild-type *Cg*Pmu1 (left) and *Cg*Pmu1 with region 3 and 4 mutations (right). The R3 amino acid clusters are coloured red (R3a) and blue (R3b) and the R4 amino acid is coloured yellow. The structures were slightly rotated to the right relative to the structures in Figures 1 and 2 so that the R3 amino acids could be visualized.

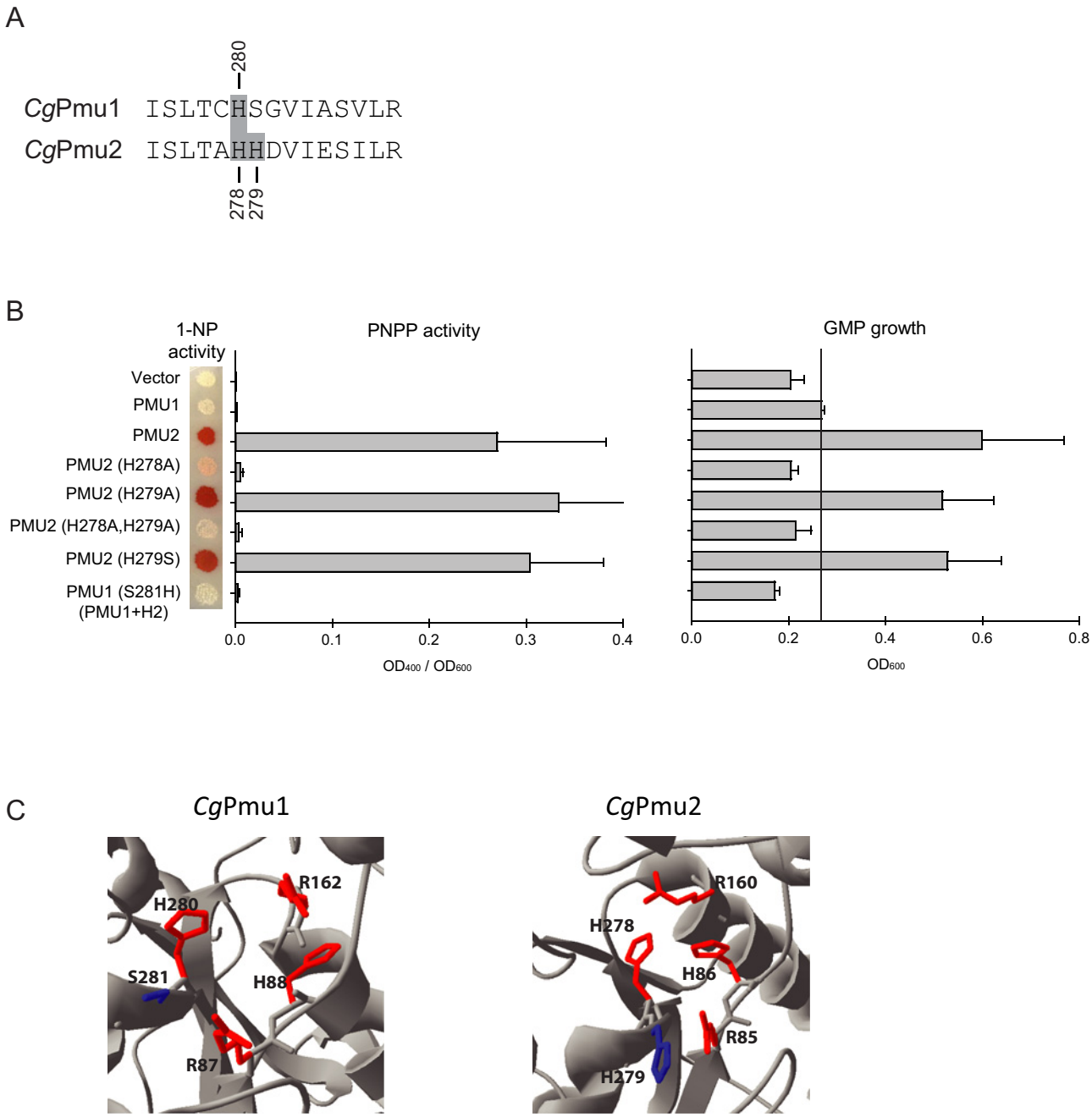

Figure 4 An additional histidine in *Cg*Pmu2, His^{279}, can partially replace the conserved active-site histidine, His^{278}

(**A**) Amino acid alignment of a region of *Cg*Pmu1 and *Cg*Pmu2, showing the conserved active-site histidine (*Cg*Pmu1 His^{280}, *Cg*Pmu2 His^{278}) in the C-terminal tail of the proteins. In *Cg*Pmu2, there is an additional histidine adjacent to the active-site histidine (*Cg*Pmu2 His^{279}). (**B**) Point mutations in the active-site amino acids of *Cg*Pmu2 and *Cg*Pmu1 with corresponding *in vivo* phosphatase activity results, measured as in Figure 2A. (**C**) Predicted active-site structures of both *Cg*Pmu1 and *Cg*Pmu2. Active site amino acid side chains are displayed in red. The adjacent histidine side chain in *Cg*Pmu2 and the corresponding serine in *Cg*Pmu1 are displayed in blue.

similar to what we observed in a single-region FUS mutant (either region 3 or 4) combined with point mutations in the other region, suggesting that the clusters of amino acid changes we identified are the main drivers of *Cg*Pmu2 phosphatase activity. None of these changes conferred *in vivo* activity against PNPP (Figure 6A), suggesting that other changes between *Cg*Pmu1 and *Cg*Pmu2 might influence the stability of the proteins in the context of the cell wall, at least when cells are incubated at pH 4.2 over the 10-min time period of the *in vivo* PNPP assay.

In total, our data indicate that amino acid changes in region 4 (R4 and H2), which may affect the structure and/or stability of the active site, appear to control the K_M or affinity of the phosphatase for substrates. Altering the active site to be more like *Cg*Pmu2 causes the affinity for G-1-P and the V_{max} for substrates GMP and PNPP to increase. Region 3 alterations (R3) appear to be required to stabilize the enzyme and enhance the activity changes observed from alterations to region 4. The alterations together recapitulate *Cg*Pmu2 activity with regards to altered affinity for G-1-P and

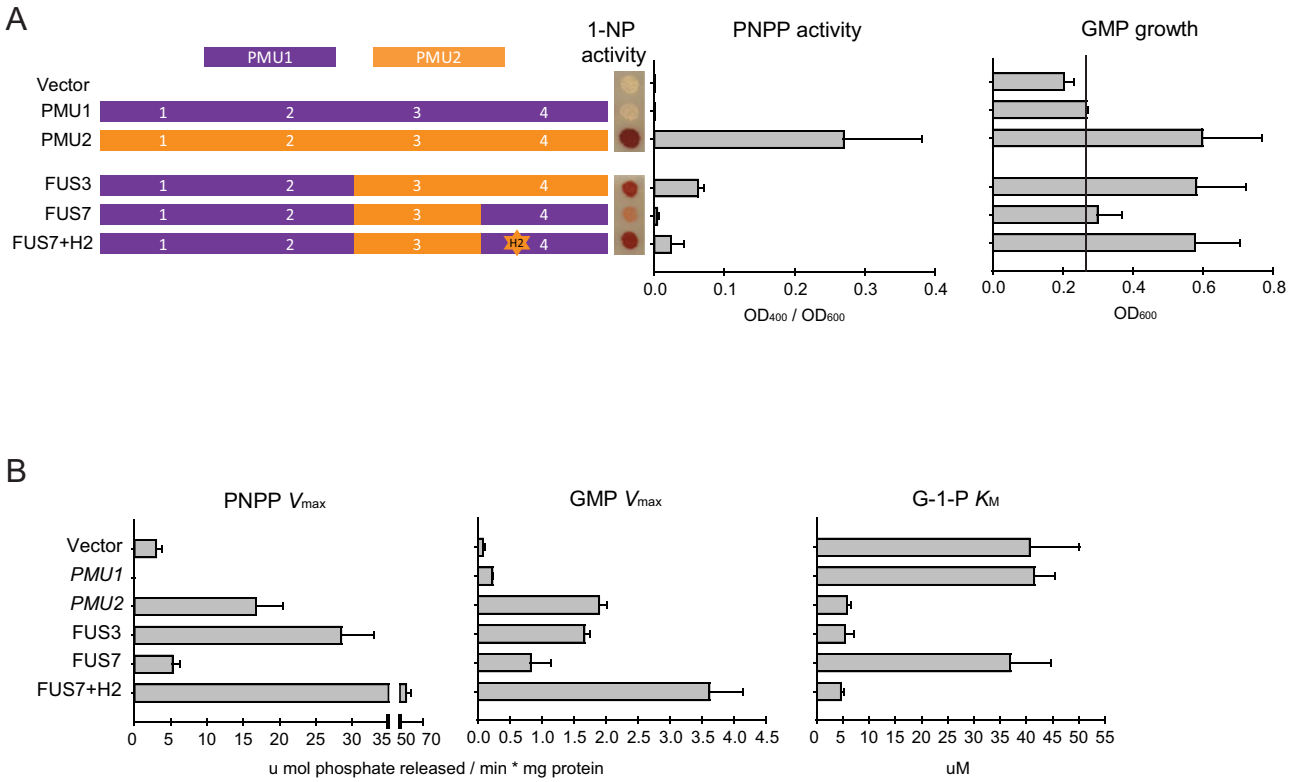

Figure 5 An additional histidine in *Cg*Pmu2, His^{279}, can confer phosphatase activity on *Cg*Pmu1

(**A**) Schematic of Pmu1-Pmu2 fusions, with corresponding *in vivo* phosphatase activity results. Introduction of an additional histidine (Pmu1 S281H) into a FUS7 background (FUS7 + H2) enhanced phosphatase activity above FUS7 alone. *In vivo* phosphatase activity was measured as in Figure 2A. (**B**) Purified proteins were incubated with various phosphate-containing substrates in *in vitro* kinetic assays and measured as in Figure 2B.

V_{max} for GMP and PNPP *in vitro*. The other ~50 amino acid changes throughout the proteins contribute to more subtle effects, such as stability. Remarkably, the R4 mutant consists of a single amino acid change A285E in *Cg*Pmu1 and it allows for utilization of phosphate from nucleotides. This amino acid change is the key to the neofunctionalization of *Cg*Pmu2 into a broad-based phosphatase and suggests that simple mutational changes in an enzyme sequence are able to change its activity towards organic phosphates.

DISCUSSION

We previously identified a cluster of three paralogues formed through gene duplication in *C. glabrata* [4]. *Cg*Pmu2 has gained a novel phosphatase activity that is not observed in the ancestral Pmu1 protein. In the present study, we divided the proteins into four regions, expressed combinations of regions of *Cg*Pmu1 and *Cg*Pmu2 as fusion proteins and determined that whereas region 3 and region 4 of *Cg*Pmu2 each, individually, had little effect on 1-NP phosphatase activity, their combination enhanced phosphatase activity. We performed additional *in vivo* and *in vitro* phosphatase assays with various substrates and paired the fusions with one or more point mutations. We identified clusters of amino acids in regions 3 and 4 of the enzyme that were able to confer phosphatase activity on *Cg*Pmu1 in various combinations.

Results from the various assays for a particular fusion protein were often consistent for different substrates, but there were some differences. Most of the inconsistencies are most probably due to structure differences between the various substrates; it is reasonable to assume that point mutations in the *Cg*Pmu1 enzyme may lead to changes in its ability to recognize or cleave phosphate off of one or more specific substrates. We have previously determined through *in vitro* kinetic assays that *Cg*Pmu1 and *Cg*Pmu2 differ in their binding affinity and/or enzymatic activity for different substrates [4]. However, the most glaring difference observed, between the *in vivo* and the *in vitro* PNPP assays, was confusing because the substrate is the same in both assays. For example, regions 3 or 4 from *Cg*Pmu2 in a *Cg*Pmu1 background (FUS7 and FUS5 respectively) did not exhibit any PNPP activity in the *in vivo* assay, but expressed as much enzymatic activity as full-length *Cg*Pmu2 against PNPP in an *in vitro* assay (Figures 2A and 2B). This discrepancy is most probably due to the difference in how the assays are performed and the microenvironment in which each enzyme functions. The *in vitro* assays consist of incubation with substrate in a pH buffered solution with purified enzyme, which means little interference from other cellular proteins/enzymes. The *in vivo* PNPP assay consists of incubation with a substrate, but the enzyme is expressed in the periplasmic space in a cellular context and needs to function in the presence of other cellular enzymes/proteases. One possibility is that the mutants that do not show activity in the *in vivo* PNPP assay are incorrectly folded in the periplasmic space. However, this is unlikely because many do show *in vivo* activity against GMP. It is more likely that the protocol for the *in vivo* GMP assay is less demanding of the enzyme than the PNPP assay; the cells are grown overnight on GMP and so even if there is a low level of activity in a mutant due to interference from cellular enzymes, it

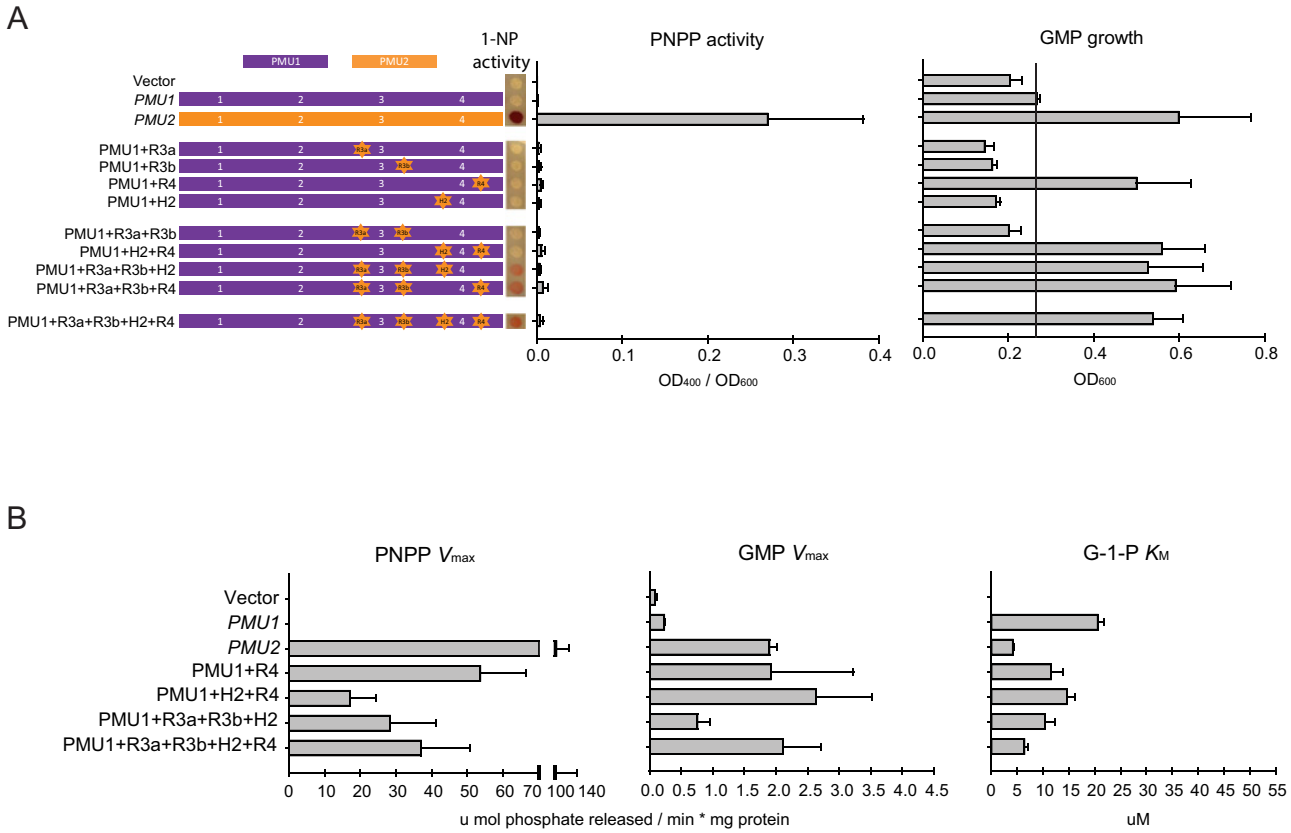

Figure 6 Combinations of region 3 and 4 point mutations are sufficient to confer phosphatase activity on *Cg*Pmu1

(**A**) Schematic of point mutations introduced to *Cg*Pmu1, with corresponding *in vivo* phosphatase activity results, which were measured as in Figure 2A. Introduction of region 3 mutants (R3a and R3b) in combination with one or both of the region 4 mutants (H2 and R4) greatly increased the broad-spectrum phosphatase activity of the protein. (**B**) Purified proteins were incubated with various phosphate-containing substrates in *in vitro* kinetic assays and measured as in Figure 2B. Only the R4 mutant was able to enhance *in vitro* phosphatase activity on its own.

will still cleave enough GMP over the course of 24 h to exhibit a clear difference in growth compared with *Cg*Pmu1. Therefore, the lack of activity of some of the fusions/mutants in the *in vivo* PNPP assays is most probably due to differences in stability compared with full-length *Cg*Pmu2; enough amino acids are changed to allow the enzyme to function *in vitro*, but it is not quite stable enough to work efficiently within the microenvironment of the periplasmic space.

The amino acids in region 3 that conferred enhanced phosphatase activity mapped to two clusters within region 3 of the enzyme (Figure 3C: R3a and R3b). The clusters were found in a region of the protein structure with low order and side chains from each cluster face toward the other cluster. Conversion of both clusters to the amino acids found in *Cg*Pmu2 was necessary for the increase in enzymatic activity. Therefore, it is likely that individual amino acid changes in region 3 may have accumulated for a long time before enough changes occurred to allow for neofunctionalization.

In contrast with the region 3 mutant clusters, conversion of both region 4 clusters (R4 and H2) was not necessary in order to recapitulate the phosphatase activity of the region 4 fusion. Each region 4 mutant was able to confer enhanced phosphatase activity and the two did not have an additive effect when combined. The R4 mutant is within an α-helix very near the active site and H2 is the histidine adjacent to the active site histidine and forms the beginning of this same α-helix. Perhaps, altering one or both the side chains alters the orientation of the α-helix so that the active site amino acids may better interact with the substrate. However, in the predicted *Cg*Pmu1 and *Cg*Pmu2 structures, the α-helices and active site histidines seem to be similarly aligned (Figure 1C), suggesting it may be the side chains themselves that affect phosphatase activity. Both amino acid replacements represent a change in size and charge of the side chain, so they may affect the stability of substrate binding in the enzyme-active-site pocket.

Most members of the superfamily, even those categorized as phosphomutases, are probably also able to act as phosphatases [11,21,22]. Mutases work by pulling a phosphate off a substrate (just like a phosphatase), but holding on to the phosphate long enough to reorient the substrate and attach the phosphate on to a new position on the substrate [11]. Therefore, slight adjustments in the ability to hold on to the substrate may push the enzyme away from mutase-like activity and toward phosphatase-like activity. One example of this is the removal of the C-terminal seven residues from dPGM in *S. cerevisiae*; the enzyme lost mutase activity but retained phosphatase activity [21]. The hypothesis, which was strengthened when a higher-resolution crystal structure was published a few years later, was that the C-terminal domain stabilizes the intermediate phosphorylated form in order to enhance mutase activity [22]. In further support of this hypothesis are our previous *in vitro* enzymatic assays, which determined that all three *Cg*Pmu proteins have some phosphatase activity against a small number of substrates but that only *Cg*Pmu2 has high catalytic rates of phosphatase activity against a number of

substrates [4]. In our experiment, perhaps the adjacent histidine and the R4 mutant amino acid may alter the active site in order to push the activity away from the mutase-like function of *Cg*Pmu1 and towards a phosphatase-like activity. This would support the established theory that 'promiscuous enzymes' (enzymes that may have additional functions from their most well-known function and multiple substrates) are key drivers of evolution, especially during gene duplication/neofunctionalization [23–25].

The two histidines and two arginines that form the catalytic core are completely conserved across all known active members of the superfamily of histidine phosphatases. The first histidine is thought to be the side chain that is actually phosphorylated during the reaction (it physically removes the phosphate from the substrate), whereas the second histidine and the two arginines stabilize the negatively-charged phosphate [11]. In the present study, we found that *Cg*Pmu2 retained residual 1-NP phosphatase activity when it lost the second active-site histidine (His^{279}), suggesting that it is not essential for enzymatic activity (Figure 4B). This is a novel finding; whenever these four active-site amino acids are mutated to alanine in the literature, the mutations have resulted in nearly complete loss of enzyme activity [11,26]. There is one exception in the literature: mutation of the first or second active-site histidines in rat fructose 2,6-bisphosphate only reduced enzymatic activity to 17 % and 12 % respectively, whereas deletion of both histidines completely eliminated enzymatic activity [27]. The authors hypothesized that when the second histidine is mutated, another amino acid in the active site is able to partially take over its function [27]. In our experiment, additional deletion of the adjacent histidine (His^{279}) was able to completely abolish the residual activity left over in the *Cg*Pmu2 H278A mutant, suggesting it was partially taking over when the active site histidine was absent (Figure 4B). Therefore, the adjacent histidine seems to have two separate roles: when the active site histidine is present in fusions of *Cg*Pmu1-*Cg*Pmu2, addition of H2 can greatly enhance phosphatase activity of the fusion protein and when the active site histidine is mutated to alanine in full-length *Cg*Pmu2, H2 can partially take over its catalytic role in the active site. The latter role is most probably due to H2 directly replacing the missing active-site histidine in the catalytic phosphatase reaction. The former role may be more generally due to an adjustment in active site structure or flexibility, leading to a shift in enzymatic activity and/or substrate specificity. Since this adjacent histidine is not found in any other members of the histidine phosphatase superfamily, it is a novel substitution that, in addition to the R3 and R4 amino acid clusters, has allowed *Cg*Pmu2 to take over the role of the missing Pho5 protein in *C. glabrata*.

Finally, the region 4 substitution (R4) represents a single point mutation (A285E) and this single amino acid change significantly enhanced phosphatase activity against various substrates in a FUS7 background as well as a R3 mutant background. Interestingly, this single amino acid change by itself was able to confer growth in GMP nearly to the same level as full-length *Cg*Pmu2 and raised the V_{max} of the enzyme against PNPP and GMP to nearly that of full-length *Cg*Pmu2 (Figures 6A and 6B, PMU1 + R4). This neofunctionalization demonstrates that a single amino acid change provides flexibility in substrate specificity for an organism, which could allow it to respond to changes in nutrient sources in its environment.

AUTHOR CONTRIBUTION

Kelly Orlando, Danielle Davies and Dennis Wykoff conceived the project and all authors, including Sarah Leone, generated data for the manuscript. Kelly Orlando, Christine Iosue and Dennis Wykoff wrote the manuscript.

ACKNOWLEDGEMENTS

The authors thank Michael Cirullo for assistance with measurements of PNPP activity *in vivo* and feedback from members of the department of biology at Villanova University, especially Daniel Kraut.

FUNDING

This work was supported by the National Science Foundation [grant numbers MCB-1121714 and MCB-1412582]; the Dennis M. Cook Endowed Gregor Mendel Chair in Genetics Endowment; the Villanova College of Liberal Arts and Sciences; and the Villanova Department of Biology.

REFERENCES

1 Penido, M.G. and Alon, U.S. (2012) Phosphate homeostasis and its role in bone health. Pediatr. Nephrol. **27**, 2039–2048 CrossRef PubMed
2 Ljungdahl, P.O. and Daignan-Fornier, B. (2012) Regulation of amino acid, nucleotide, and phosphate metabolism in *Saccharomyces cerevisiae*. Genetics **190**, 885–929 CrossRef PubMed
3 Springer, M., Wykoff, D.D., Miller, N. and O'Shea, E.K. (2003) Partially phosphorylated Pho4 activates transcription of a subset of phosphate-responsive genes. PLoS Biol. **1**, E28 CrossRef PubMed
4 Orkwis, B.R., Davies, D.L., Kerwin, C.L., Sanglard, D. and Wykoff, D.D. (2010) Novel acid phosphatase in *Candida glabrata* suggests selective pressure and niche specialization in the phosphate signal transduction pathway. Genetics **186**, 885–895 CrossRef PubMed
5 Gabaldon, T., Martin, T., Marcet-Houben, M., Durrens, P., Bolotin-Fukuhara, M., Lespinet, O., Arnaise, S., Boisnard, S., Aguileta, G., Atanasova, R. et al. (2013) Comparative genomics of emerging pathogens in the *Candida glabrata* clade. BMC Genomics **14**, 623 CrossRef PubMed
6 Kerwin, C.L. and Wykoff, D.D. (2009) Candida glabrata PHO4 is necessary and sufficient for Pho2-independent transcription of phosphate starvation genes. Genetics **182**, 471–479 CrossRef PubMed
7 Elliott, B., Haltiwanger, R.S. and Futcher, B. (1996) Synergy between trehalose and Hsp104 for thermotolerance in *Saccharomyces cerevisiae*. Genetics **144**, 923–933 PubMed
8 Hurlimann, H.C., Laloo, B., Simon-Kayser, B., Saint-Marc, C., Coulpier, F., Lemoine, S., Daignan-Fornier, B. and Pinson, B. (2011) Physiological and toxic effects of purine intermediate 5-amino-4-imidazolecarboxamide ribonucleotide (AICAR) in yeast. J. Biol. Chem. **286**, 30994–31002 CrossRef PubMed
9 Rebora, K., Laloo, B. and Daignan-Fornier, B. (2005) Revisiting purine-histidine cross-pathway regulation in *Saccharomyces cerevisiae*: a central role for a small molecule. Genetics **170**, 61–70 CrossRef PubMed
10 Kerwin, C.L. and Wykoff, D.D. (2012) *De novo* generation of a phosphate starvation-regulated promoter in *Candida glabrata*. FEMS yeast Res. **12**, 980–989 CrossRef PubMed
11 Rigden, D.J. (2008) The histidine phosphatase superfamily: structure and function. Biochem. J. **409**, 333–348 CrossRef PubMed
12 Corrigan, M.W., Kerwin-Iosue, C.L., Kuczmarski, A.S., Amin, K.B. and Wykoff, D.D. (2013) The fate of linear DNA in *Saccharomyces cerevisiae* and *Candida glabrata*: the role of homologous and non-homologous end joining. PLoS One **8**, e69628 CrossRef PubMed
13 Sikorski, R.S. and Hieter, P. (1989) A system of shuttle vectors and yeast host strains designed for efficient manipulation of DNA in *Saccharomyces cerevisiae*. Genetics **122**, 19–27 PubMed
14 Wykoff, D.D., Rizvi, A.H., Raser, J.M., Margolin, B. and O'Shea, E.K. (2007) Positive feedback regulates switching of phosphate transporters in *S. cerevisiae*. Mol. Cell **27**, 1005–1013 CrossRef PubMed
15 Huang, S. and O'Shea, E.K. (2005) A systematic high-throughput screen of a yeast deletion collection for mutants defective in PHO5 regulation. Genetics **169**, 1859–1871 CrossRef PubMed
16 Chen, P., Toribara, T. and Warner, H. (1956) Microdetermination of phosphorus. Anal. Chem. **28**, 1756–1758
17 Kelley, L.A. and Sternberg, M.J. (2009) Protein structure prediction on the Web: a case study using the Phyre server. Nat. Protocols **4**, 363–371 CrossRef
18 Jedrzejas, M.J., Chander, M., Setlow, P. and Krishnasamy, G. (2000) Structure and mechanism of action of a novel phosphoglycerate mutase from *Bacillus stearothermophilus*. EMBO J. **19**, 1419–1431 CrossRef PubMed
19 Mikhailik, A., Ford, B., Keller, J., Chen, Y., Nassar, N. and Carpino, N. (2007) A phosphatase activity of Sts-1 contributes to the suppression of TCR signaling. Mol. Cell **27**, 486–497 CrossRef PubMed

20 Rigden, D.J., Mello, L.V., Setlow, P. and Jedrzejas, M.J. (2002) Structure and mechanism of action of a cofactor-dependent phosphoglycerate mutase homolog from *Bacillus stearothermophilus* with broad specificity phosphatase activity. J. Mol. Biol. **315**, 1129–1143 CrossRef PubMed
21 Walter, R.A., Nairn, J., Duncan, D., Price, N.C., Kelly, S.M., Rigden, D.J. and Fothergill-Gilmore, L.A. (1999) The role of the C-terminal region in phosphoglycerate mutase. Biochem. J. **337** Pt 1, 89–95 CrossRef PubMed
22 Bond, C.S., White, M.F. and Hunter, W.N. (2002) Mechanistic implications for *Escherichia coli* cofactor-dependent phosphoglycerate mutase based on the high-resolution crystal structure of a vanadate complex. J. Mol. Biol. **316**, 1071–1081 CrossRef PubMed
23 Taylor, J.S. and Raes, J. (2004) Duplication and divergence: the evolution of new genes and old ideas. Annu. Rev. Genetics **38**, 615–643 CrossRef
24 Conant, G.C. and Wolfe, K.H. (2008) Turning a hobby into a job: how duplicated genes find new functions. Nat. Rev. Genet. **9**, 938–950 CrossRef PubMed
25 Khersonsky, O. and Tawfik, D.S. (2010) Enzyme promiscuity: a mechanistic and evolutionary perspective. Annu. Rev. Biochem. **79**, 471–505 CrossRef PubMed
26 Tauler, A., Lin, K. and Pilkis, S.J. (1990) Hepatic 6-phosphofructo-2-kinase/fructose-2,6-bisphosphatase. Use of site-directed mutagenesis to evaluate the roles of His-258 and His-392 in catalysis. J. Biol. Chem. **265**, 15617–15622 PubMed
27 Mizuguchi, H., Cook, P.F., Tai, C.H., Hasemann, C.A. and Uyeda, K. (1999) Reaction mechanism of fructose-2,6-bisphosphatase. A mutation of nucleophilic catalyst, histidine 256, induces an alteration in the reaction pathway. J. Biol. Chem. **274**, 2166–2175 CrossRef PubMed
28 Waterhouse, A.M., Procter, J.B., Martin, D.M., Clamp, M. and Barton, G.J. (2009) Jalview Version 2–a multiple sequence alignment editor and analysis workbench. Bioinformatics **25**, 1189–1191 CrossRef PubMed
29 Guex, N. and Peitsch, M.C. (1997) SWISS-MODEL and the Swiss-PdbViewer: an environment for comparative protein modeling. Electrophoresis **18**, 2714–2723 CrossRef PubMed

Received 27 May 2015/10 August 2015; accepted 12 August 2015
Accepted Manuscript online 12 August 2015, doi:10.1042/BJ20150611